Materials and Design 58 (2014) 346–356

Contents lists available at ScienceDirect

Materials and Design

journal homepage: www.elsevier.com/locate/matdes

Corrosion evaluation of multi-pass welded nickel–aluminum bronze alloy in 3.5% sodium chloride solution: A restorative application of gas tungsten arc welding process

Behnam Sabbaghzadeh [a], Reza Parvizi [a], Ali Davoodi [b,*], Mohammad Hadi Moayed [a]

[a] Department of Materials and Metallurgical Engineering, Faculty of Engineering, Ferdowsi University of Mashhad, 91775-1111, Iran
[b] Department of Materials and Polymer Engineering, Faculty of Engineering, Hakim Sabzevari University, Sabzevar 391, Iran

ARTICLE INFO

Article history:
Received 15 October 2013
Accepted 10 February 2014
Available online 18 February 2014

Keywords:
Gas tungsten arc welding
Nickel–aluminum bronze
Galvanic corrosion
EIS

ABSTRACT

In this research, the corrosion behavior of a gas tungsten arc welded nickel–aluminum bronze (NAB) alloy is investigated by DC and AC electrochemical techniques in 3.5% sodium chloride solution. Regarding the electrochemical impedance spectroscopy and potentiodynamic results, uniform corrosion resistance of instantly immersed weld and base samples are almost analogous and increased (more in weld region) during the immersion times. Moreover, zero resistant ammeter results demonstrated that the few nano-ampere galvanic currents are attributed to microstructural and morphological differences between these two regions. Therefore, the welding procedure could not deteriorate the general corrosion resistance of the restored damaged NAB parts operating in marine environments.

1. Introduction

Nickel–aluminum bronze (NAB) alloys containing 9–12% (wt.%) aluminum with additions of up to 6% (wt.%) of iron and nickel, represent one of the most important groups of commercial aluminum bronzes. As the major alloying element, aluminum content would result in higher strength and improve the corrosion resistance (by formation of an oxide/hydroxide film) and castings/hot working properties. On the other side, nickel also improves corrosion resistance, strength and stabilises the microstructure while iron refines grains and increases the alloy tensile strength [1,2]. Both cast and wrought aluminum bronze compounds offer a good combination of mechanical properties and corrosion resistance. Consequently, aluminum bronzes have been widely used for decades in a variety of marine or saline environments including valves, fittings, ship propellers, pump castings, pump shafts, valve stems and heat exchanger water boxes [2–4]. However, these alloys can suffer from localized corrosion (e.g. pitting, crevice, etc.) especially in flow conditions [5]. NAB alloys are metallurgical complex alloys with several intermetallic phases such as α, β', κ_i, κ_{ii}, κ_{iii} and κ_{iv} in which small variations in composition can result in development of markedly different microstructures. This can also lead to extensive changes of alloy corrosion resistance in seawater. The microstructures that can result in an optimum corrosion resistance can be obtained by controlling the composition and the heat treatment procedure [1]. Wharton et al. used five types of NAB alloys (as-cast and wrought) with different compositions and heat treatment (annealing) backgrounds and compared their corrosion behaviors through various electrochemical techniques [1]. They reported that the cast/annealed samples represented higher corrosion current densities in compared to wrought samples in seawater [1]. However, NABs are the most corrosion resistant types of copper-based alloys to flow-induced corrosion [5,6]. Their resistance has been attributed to a thin protective layer, containing aluminum and copper oxides [7,8]. Due to the presence of stable intermetallic compounds in NAB and the α/β phase boundary that is near the solidus line, it is very difficult to homogenize these alloys at their solid state and thus, a welding approach can be performed for this aim [9]. Indeed, this is a crucial matter whenever an inevitable industrial assembling process such as welding operation is carried out.

Alternatively, some defects and cracks can be induced by cavitation, de-alloying, stress corrosion cracking, pitting and erosion–corrosion mechanisms in some parts of NAB alloys (e.g. impellers), after long exposure times to seawater [10–14]. For instance, Alfantazi et al. reported that for a couple of copper alloys in 1 M NaCl solution (pH = 6), the samples experienced a general dissolution mechanism at higher overpotentials and did not suffer from localized corrosion while at more alkaline pH conditions, they revealed a type of passivity (and passivity breakdown) behavior in

* Corresponding author. Tel./fax: +98 5714003520.
E-mail address: a.davoodi@hsu.ac.ir (A. Davoodi).

http://dx.doi.org/10.1016/j.matdes.2014.02.019
0261-3069/

potentiodynamic results [2]. Also, Ni et al. showed that the NAB samples had finer and more homogenous microstructure (after performing a friction stir process) in comparison with the unprocessed alloy and that resulted in better corrosion resistance [15]. Furthermore, the namely materials can suffer surface damage under conditions of extreme flow velocity or fluid disturbance [5]. Since replacement of these parts with exactly the same material is very expensive, welding operation could be an economical method for restoration of NAB parts. Meanwhile, this method may lead to severe corrosion attacks due to occurrence of galvanic couples between weld and base alloy zones. However, there have been few studies committed to corrosion investigation of welded NAB alloys. For example, Ni et al. have employed the friction stir processing as a technique to modify the microstructure of the NAB alloys and have investigated the general corrosion properties of the surface processed NAB alloy [15]. Xiao-ya et al. also studied the cavitation behavior of NAB welds and showed that this type of corrosion initiates at the phase boundaries [16].

The aim of this research is devoted to assess the general and galvanic corrosion behavior of multi-pass gas tungsten arc (GTA) welded nickel–aluminum bronze (C95800) plates by DC and AC electrochemical techniques in aerated 3.5% (wt.%) sodium chloride solution. On the basis of ZRA measurement, a clear picture of the mechanism responsible for galvanic corrosion between the base and weld regions is presented. Finally, it will be inferred from the results whether this specified operation can be employed on the restored NAB alloys.

2. Materials and methods

Two as-cast NAB (C95800) plates were used as welding materials. The chemical composition (in wt.%) of the alloy was determined by quantometery method as 9.14% Al, 4.75% Ni, 3.1% Fe, 0.75% Mn and Cu as balance. U-shape groove of alloy plates with 10 mm in thickness and 100 mm in both length and width were joined using a multi-pass GTAW process. Argon gas, as shielding gas, was continuously purged during the four welding passes. The filler metal was ERCuNiAl that was chosen due to AWS A5.7 standard in the proposed nominal composition range (in wt.%) of 8.5–9.5% Al, 4–5.5% Ni, 3–5% Fe, 0.6–3.5% Mn, 0.1% Zn, 0.1% Si, 0.02% Pb, 0.5% of other elements and Cu as balance. The mean values of AC welding current and voltage were 220 A and 22 V, respectively. After completion of the welding operations, the weldments were cooled in air. Identical, in surface area, specimens with ca 0.203 cm^2 in cross section were extracted from the base and weld zones; see Fig. 1. Due to excessive conductivity of copper alloys and thus narrowness of the heat affected zone (HAZ), it was impossible to extract an individual sample from this zone. In order to examine the corrosion properties, the samples were cold mounted using a self-cure epoxy resin in cylindrical molds after an electrical connection was made between the sample and a copper wire. For corrosion and microstructural investigations, the samples were ground up to 1200 SiC abrasive paper, polished using 1 μm diamond paste, degreased by ethanol, washed by distilled water and finally dried by hot air. Prior to corrosion experiments, microstructural evaluations on individual parts of the prepared samples were performed using an Olympus optical microscopy (OM). The etchant used for metallographic examinations was prepared by mixing 8 g of ferric chloride, 25 ml of hydrochloric acid and 100 ml of distilled water in a glass beaker [17]. The corrosion properties of the base and weld regions were studied on individual samples by monitoring potentiodynamic polarization (PDP), electrochemical impedance spectroscopy (EIS) and zero resistant ammeter (ZRA). All corrosion experiments were done in aerated (exposed to air) 3.5 wt.% sodium chloride solution (prepared from distilled water and analytical Merck grade sodium chloride) with pH of 6.8 and at room temperature. Former to all corrosion measurements, each specimen was held at its rest potential for about 15 min to reach an stable corrosion potential. All electrochemical measurements were performed using an ACM instrument potentiostat (AC Gill No. 1380). A three electrode configuration was used for electrochemical measurements including platinum wire as the counter, saturated calomel as the reference and prepared specimens as the working electrodes, respectively. It should be noted that all potentials were measured and plotted against saturated calomel reference electrode (SCE). For PDP measurements, the potential was scanned from −400 to 1500 mV (vs. SCE) at 1 mV/s scanning rate. In order ot extract polarization parameters from PDP curves, Tafel extrapolation method was used. In order to study the galvanic couple (couple potentials and current densities) between these two identical (in surface area) samples (with 2–3 cm distance in between), zero resistant ammeter (ZRA) test was performed at 0, 24, 48 and 72 h of immersion. The galvanic current density (i_{couple}) and galvanic potential (E_{couple}) were recorded simultaneously as a function of time i.e. 900 s applying a zero potential against the galvanic cell. The current density was calculated by dividing the measured current to the area of the electrode. EIS test was also performed in the frequency range of 30,000–0.01 Hz with a potential amplitude of ±15 mV. The aim was to characterize and compare the surface evolution of instantly immersed (0 h) and 72 h immersed samples in three different applied overpotentials; 0 and ±100 mV (vs. SCE) with respect to each sample corrosion potential. The EIS results were analyzed and the equivalent circuits parameters were extracted by using the EIS spectrum analyzer software. Note that for checking the reproducibility of the electrochemical experiments, each of the corrosion tests was repeated for at least three times. Finally, the most representative data that was closest to the reported average values were selected for plotting.

3. Results and discussion

3.1. Microstructure characterization

Fig. 2 shows the microstructures and morphologies of the base and weld regions provided by OM. The image with lower magnification clearly reveals the sharp interface between these two regions (base and weld); see Fig. 2a. Base metal can be observed at the left

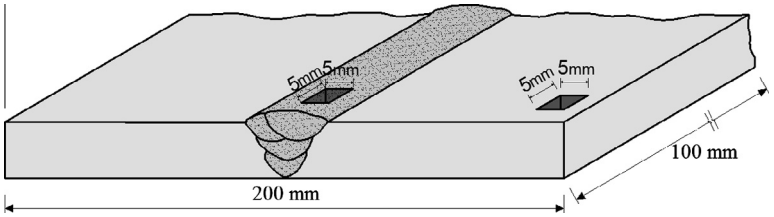

Fig. 1. Schematic illustration of the performed four-pass GTA welding procedure and the samples extraction sites from distinct base and weld regions.